Dispersion and Mechanical Properties of a Nanocomposite with an Organoclay in an Ionomer-Compatibilized LDPE Matrix

P. Santamaría, J. I. Eguiazabal, J. Nazabal

Departamento de Ciencia y Tecnología de Polímeros and Instituto de Materiales Poliméricos "POLYMAT", Facultad de Ciencias Químicas UPV/EHU, PO Box 1072, 20080 San Sebastián, Spain

Received 30 March 2010; accepted 25 May 2010
DOI 10.1002/app.32877
Published online 20 August 2010 in Wiley Online Library (wileyonlinelibrary.com).

ABSTRACT: Widely dispersed low density polyethylene (LDPE) based nanocomposites (Nc's) were obtained in the melt state thanks to their compatibilization with a zinc ionomer of poly(ethylene-*co*-methacrylic acid) (Pema-Zn). The variables probed were the ionomer and organoclay content ranging from 0 to 20%, and from 0 to 10%, respectively. The TEM images showed that the organoclay is widely exfoliated. Furthermore, we report for the first time that the organoclay is concentrated in irregular zones. Taking into account the compatibility between MMT and the ionomer, it is plausible that the ionomer clusters are also concentrated in the organoclay-rich regions. This heterogeneous microstructure has a positive effect on the mechanical properties since the Nc's are ductile, and the modulus increases were among the largest reported for LDPE, attaining a 160% increase with a 10% montmorillonite (MMT) content. © 2010 Wiley Periodicals, Inc. J Appl Polym Sci 119: 1762–1770, 2011

Key words: nanocomposites; polyethylene (PE); compatibilization; ionomer; mechanical properties

INTRODUCTION

Nc's based on a polymeric matrix reinforced with dispersed laminar and organically modified silicates such as OMMT, constitute nowadays an area of growing importance in polymeric materials from both a fundamental and an applied standpoint.[1,2] Thanks to widespread research efforts, some of the most technologically relevant polymers have been successfully used as matrices for Nc's when mixed in the melt state with the appropriate organoclay. This has lead to enhanced material properties, particularly to modulus increases, that depend on the dispersion level attained,[3–5] and that are always far superior than their microcomposite analogues.

Several techniques can be employed when this simple blending process does not yield the desired organoclay dispersion. The use of a fully dispersed masterbatch of a polymer miscible with the desired matrix[6–10] is one of the techniques used, for instance, to obtain exfoliated PA6.6 Nc's from a PA6 based masterbatch.[7] However, the method most commonly used is the chemical modification of the matrix to render it more compatible with the organically modified clay. The modification of the matrix can be done either directly,[11,12] or by addition of small amounts of conveniently modified matrix.[13]

In the case of polyolefins, the technique used most often is the addition of small amounts of polyolefin matrix grafted with maleic anhydride (MA).[14–18] The presence of MA modifies the nonpolar nature of the matrix rendering it more compatible with the organoclays. Other less frequently used techniques are, for example, the addition of compatibilizers as oxidized PE,[19–22] copolymers of ethylene and both acrylic acid[23–25] and methacrylic acid,[26] EVA,[27] and a copolymer of PE with methyl acrylate.[28]

Ionomers based on a polyolefin chain modified with partially neutralized methacrylic acid may be able to compatibilize polyolefin-based Nc's because they increase the polarity of the matrix. Until now, only a preliminary work on LLDPE modified with a constant (18%) ionomer content has been published.[18] The maximum MMT content was low (4.4%), and the phase behavior of the matrix was not reported. In a previous report on the dispersion of OMMT's using a single MMT content,[29] pure Pema-Zn was shown to be more effective than the Pema-Li in dispersing organoclays. Moreover, it was shown that the Cloisite 20A organoclay was the most adequate organic modification for achieving dispersion when using this ionomer.

In this study, Nc's based on LDPE containing a MMT modified with a two-tailed surfactant (Cloisite

Correspondence to: J. I. Eguiazabal (josei.eguiazabal@ehu.es).

Contract grant sponsor: Spanish Ministerio de Ciencia e Innovación; contract grant number: MAT2007-60153.

20A) were obtained in the melt state using Pema-Zn as a compatibilizer. The variables studied were the MMT and the compatibilizer content that ranged from 0 to 10% and from 0 to 20%, respectively. The phase behavior of the Nc's was studied by differential scanning calorimetry (DSC) and dynamic mechanical analysis (DMA), their nanostructure by X-ray diffraction (XRD) and transmission electron microscopy (TEM), and their mechanical properties by stress-strain tests. The results obtained were compared with those obtained previously using other compatibilizers.

EXPERIMENTAL

Materials

The polymers used in this work were a LDPE and a zinc ionomer of poly(ethylene-*co*-methacrylic acid) (Pema-Zn). The LDPE was Dow 302E (The Dow Chemical Company). It had a melt flow index of 0.8 g/10 min, measured at 190°C and with a 2.16 kg load. The Pema-Zn was Surlyn 1652 (DuPont). It had a melt flow index of 5.2 g/10 min, measured at 190°C and with a 2.16 kg load, a 6.5 wt % methacrylic acid content and 18% neutralized. The filler was a MMT modified with a two-tailed surfactant, dimethyl bis (hydrogenated-tallow) ammonium chloride (Cloisite® 20A (20A), Southern Clay Products). It had an organic modifier content of 95 meq/100g clay and a basal spacing, d_{001}, of 2.31 nm.

Preparation of the nanocomposites

Drying before processing was performed at 65°C in vacuum for 24 h in the case of Pema-Zn. LDPE/Pema-Zn blends were firstly obtained in a twin-screw extruder kneader (Collin ZK25) (screw diameter of 25 mm, length-to-diameter ratio 30/1) at a barrel temperature of 180°C and a screw rotation speed of 200 rpm. The content of Pema-Zn in the blends was 0, 5, 10, 15, and 20% (wt/wt). Then, varying contents of 20A were added to the blends in a second extrusion step carried out under the same conditions. After extrusion, the extrudates were cooled in a water bath and pelletized. The mean residence time during materials extrusion was 50 s. The inorganic MMT content, which was measured by calcination, changed from 0 to 10%, with respect to the matrix (LDPE plus Pema-Zn) content. The Nc's will be named as *x/y* where *x* and *y* are the Pema-Zn and MMT contents, respectively.

Subsequent injection molding was carried out in a Battenfeld Plus 350/75 reciprocating screw injection molding machine to obtain tensile (ASTM D638, type IV, thickness 3.19 mm) and impact (ASTM D256, thickness 3.1 mm) specimens of the Nc's and of the reference blends. The screw of the plasticization unit was a standard screw with a diameter of 25 mm and an L/D ratio of 14. The melt temperature was 180°C and the mold temperature 18°C. The injection speed and pressure were 56.0 $cm^3 \cdot s^{-1}$ and 800 bar (80 MPa), respectively.

Characterization of the nanocomposites

The samples for calorimetric analysis (Perkin–Elmer DSC-7) were heated from 20 to 150°C at 20°C/min, held at 150°C for 1 min and subsequently cooled to 20°C at 20°C/min. After holding the samples at 20°C for 1 min, they were reheated to 150°C at 20°C/min. The crystallinity was calculated using a heat fusion for 100% crystalline polyethylene of 290.4 J/g.[30] The DMA (TA Q800) scans were obtained in bending mode at 4°C/min and 1 Hz from −50 to 110°C.

The XRD patterns were recorded (X'pert diffractometer) at 40 kV and 40 mA, using a Ni-filtered Cu-K_α radiation source. The scan speed was 0.1°/min. The TEM samples were cryogenically ultrathin-sectioned at 60–100 nm at −60°C, and observed in a Philips Tecnai G2 20 TWIN apparatus at an accelerating voltage of 200 kV.

Capillary rheometry measurements were performed at 180°C in a Göttfert Rheograph 2002 extrusion rheometer using a flat entry capillary tungsten die with an *L/D* ratio of 30/0.5.

Tensile testing (Instron 5569) was carried out in a minimum of five specimens for each reported value at a cross-head speed of 10 mm/min and at 23 ± 2°C and 50 ± 5% relative humidity. The mechanical properties (tensile strength and ductility, measured as the break strain) were determined from the load-displacement curves and the Young's modulus by extensometry at a cross-head speed of 1 mm/min.

RESULTS AND DISCUSSION

Phase behavior

The phase behavior of the Nc's was studied by both DSC and DMA. The DSC was used to study the crystalline phase, as the characteristics of the amorphous phases were more easily seen from the DMA results. Figure 1 shows the cooling DSC scans of the Nc's based on the 80/20 blend, as well as that of the blend as a reference. The trends of the scans of the Nc's with lower Pema-Zn contents were similar to those of Figure 1, but less marked. The scans of the Nc's based on the unmodified LDPE are not shown because no difference was observed between the DSC scans of the polymer and its Nc's.

As can be seen in Figure 1, the blend shows two exothermic peaks at 78 (Pema-Zn) and 96°C (LDPE), indicating the separated crystallization of Pema-Zn

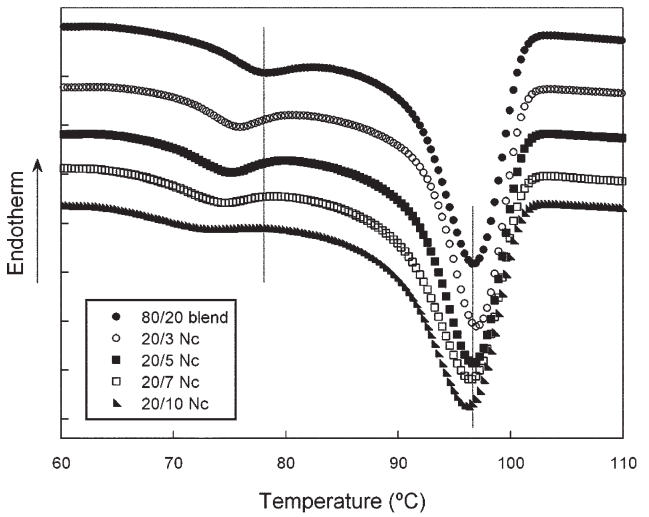

Figure 1 Cooling DSC scans of the Nc's based on the 80/20 LDPE/Pema-Zn blend with different MMT contents. The scan of the pure blend is also represented as reference.

and LDPE. In the Nc's the crystallization temperature of LDPE decreases only slightly, but that of the Pema-Zn clearly decreases. These decreases indicate a hindered crystallization that is most probably due to the presence of clay, as previously reported.[31] This hindering is more active in the case of Pema-Zn where crystallization is by itself more difficult.

The DMA scans of the Nc's with different MMT contents, as well as those of the corresponding pure blends, are shown in Figure 2(a) (90/10 blend) and Figure 2(b) (80/20 blend), respectively. The Nc's with other Pema-Zn contents showed intermediate characteristics. As can be seen, the pure blends show a main α peak at rougly 50°C that corresponds to a reorganization of the crystalline phase of the LDPE,[32,33] and a shoulder centered between -5 and -10°C that corresponds to the amorphous phase. No presence of a possible Pema-Zn-rich phase is detected. However, as its presence is difficult to detect, the DMA scans of the 80/20 LDPE/Pema-Zn blend and those of its pure components are shown in Figure 3. As can be seen, the main peak of the pure Pema-Zn, that corresponds to ionic groups,[34,35] and that is centered at 20–25°C is nearly undetected in the blend. Moreover, the position and shape of the shoulder at -5°C are the same in the LDPE and in the blend, and no additional change is seen in the blend scan. These facts deny the presence of a truly separated phase, and suggest the presence of a single amorphous phase in the blends. This conclusion is, however, a bit adventurous due to the lack of a clear T_g of the Pema-Zn. The existence of a single amorphous phase in the blends and in the Nc's will be additionally discussed in the TEM section.

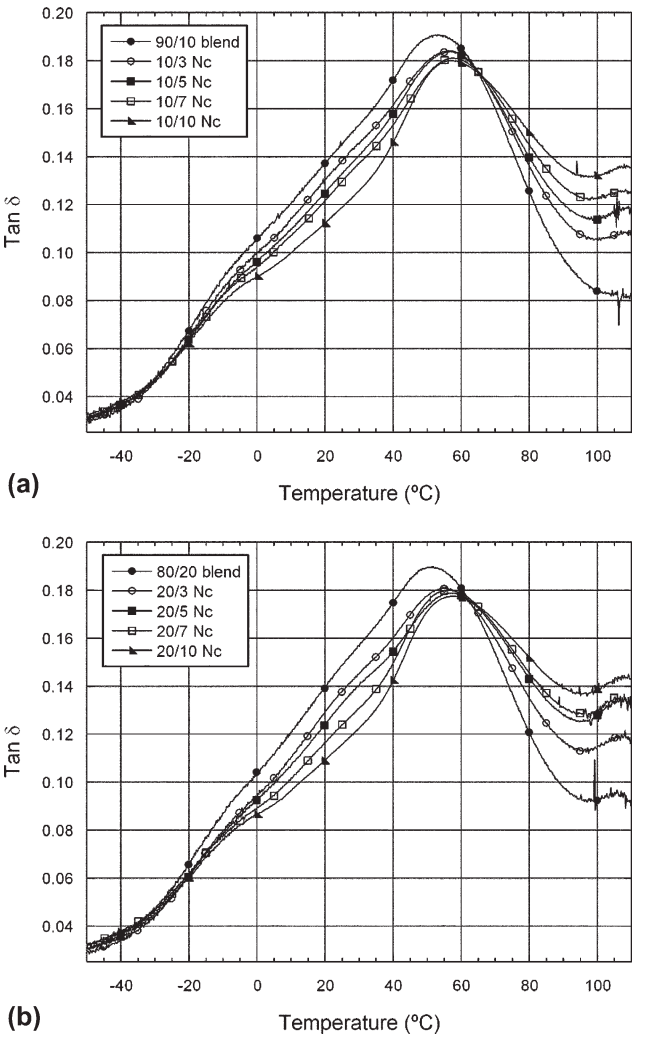

Figure 2 DMA scans of the Nc's based on 90/10 (a) and 80/20 (b) LDPE/Pema-Zn blends with different MMT contents.

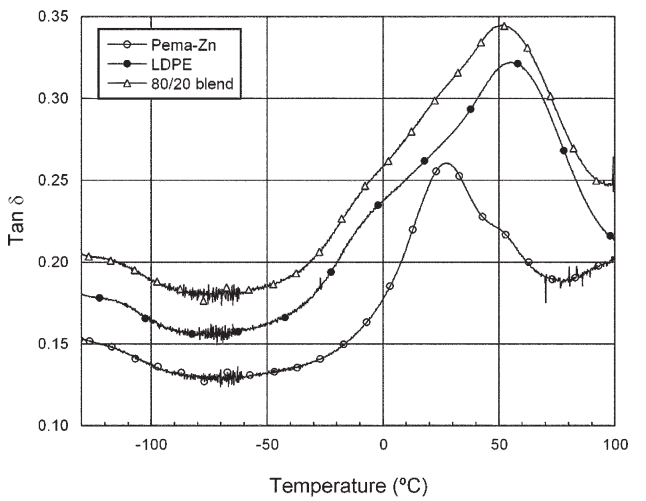

Figure 3 DMA scans of the 80/20 LDPE/Pema-Zn blend and the pure components.

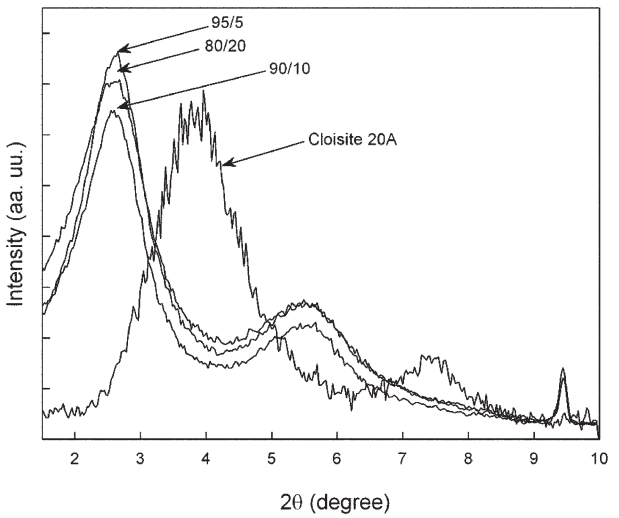

Figure 4 XRD scans of the Nc's based on 95/5, 90/10, and 80/20 LDPE/Pema-Zn blends with 3% MMT. The scan of the Cloisite 20A is represented as a reference.

Figure 3 also shows that the scan of the blend is almost parallel to that of the pure LDPE, but a slightly positive deviation appears just at the position of the main Pema-Zn peak. This indicates that in the blends many ionic groups disappeared, but some of them remained. In the scans of the Nc's of Figure 2, the positive deviation appears only at low MMT contents. At high MMT contents it is not visible due to the negative effect of the MMT presence in the tan δ zone between the main peak and the shoulder. This negative effect is seen because tan δ decreases as the MMT content increases. A similar result was seen in PC/PCL blends upon OMMT addition and was attributed to surfactant migration.[6] Although it is not shown in Figure 2, it also occurred in the case of the pure LDPE/MMT Nc's.

The position of the α peak is also seen to increase in the Nc's of Figure 2. The increase is apparently independent of the MMT content but it is slightly larger in Figure 2(b), i.e., at higher Pema-Zn contents. The increase in the α peak temperature has to be due to the presence of either Pema-Zn or MMT. To properly discuss these two options, the binary systems of LDPE with both Pema-Zn and MMT were studied by DMA. Surprisingly, neither the Pema-Zn nor the MMT presence apparently modified the position of the α peak. In bibliography, the displacements of the α peak have been attributed to exfoliated clay/LDPE interactions.[36] In this study, the LDPE based Nc's are very poorly dispersed, so MMT/matrix interactions should not exist. However, in presence of Pema-Zn the MMT can be dispersed and, therefore, it can interact with the matrix and increase the α peak temperature of the ternary systems. Therefore, supposing that the MMT is rather dispersed, the increase in the Tα of the Nc's is attributed to interactions with the MMT.

Nanostructure

The nanostructure of the Nc's was studied by both XRD and TEM. Figure 4 shows the XRD scans of the Nc's with 3% MMT, as well as that of the Cloisite 20A as a reference. Similar results were observed in the Nc's with other MMT contents. This is seen in Table I, where the Δd_{001} of all the Nc's are shown. As can be seen in Table I, intercalation was low in the case of the Nc's with a pure LDPE matrix, and much higher in the case of the compatibilized Nc's. Moreover, the Δd_{001} values did not depend on the MMT content, as had been observed in previous works.[37,38] More importantly, Δd_{001} was also independent of the Pema-Zn content, provided some Pema-Zn was present (see Fig. 4); this indicates that low modifier contents (5%) are enough for intercalation to be more effective. Thus, as has been observed in other works on Nc's,[16,19,39] the effect of the modifier is seen not only in the level of dispersion (where it is proven to work), but in the intercalation ability as well. This is probably due to interactions between the polar and ionic groups of the Pema-Zn and the polar surface of the clay not covered by the surfactant.

Large scale TEM micrographs of the Nc's with 10% MMT, and with 0, 10, and 20% Pema-Zn are shown in Figure 5. Higher magnification TEM micrographs of a typical domain present in the Nc's is shown in Figure 6. Let us consider first the possible presence of a Pema-Zn rich phase not clearly deduced up to now. If such a phase indeed existed, the MMT would be expected to be present in this phase due to its much larger compatibility with Pema-Zn. However, the shape of the domains where the MMT is concentrated is far [see Fig. 6(a)] from the roughly spherical particles characteristic of a dispersed polymeric phase. Therefore, the MMT is not located inside a Pema-Zn dispersed phase. Moreover, the facts (i) that the viscosity of the Pema-Zn and the LDPE are similar, (ii) that most of Pema-Zn is PE, and (iii) that the Pema-Zn content of the Nc's is low, are not consistent with the large particle size observed by TEM (2–3 μm). These facts indicate that a dispersed Pema-Zn-rich phase does not exist and,

TABLE I
Δd_{001} (nm) of all the Studied Nc's

	LDPE	95/5	90/10	80/20
3% MMT	0.52	1.07	1.09	1.14
5% MMT	0.39	0.91	1.00	1.03
7% MMT	0.39	0.88	0.97	0.97
10% MMT	0.37	0.83	0.85	0.97

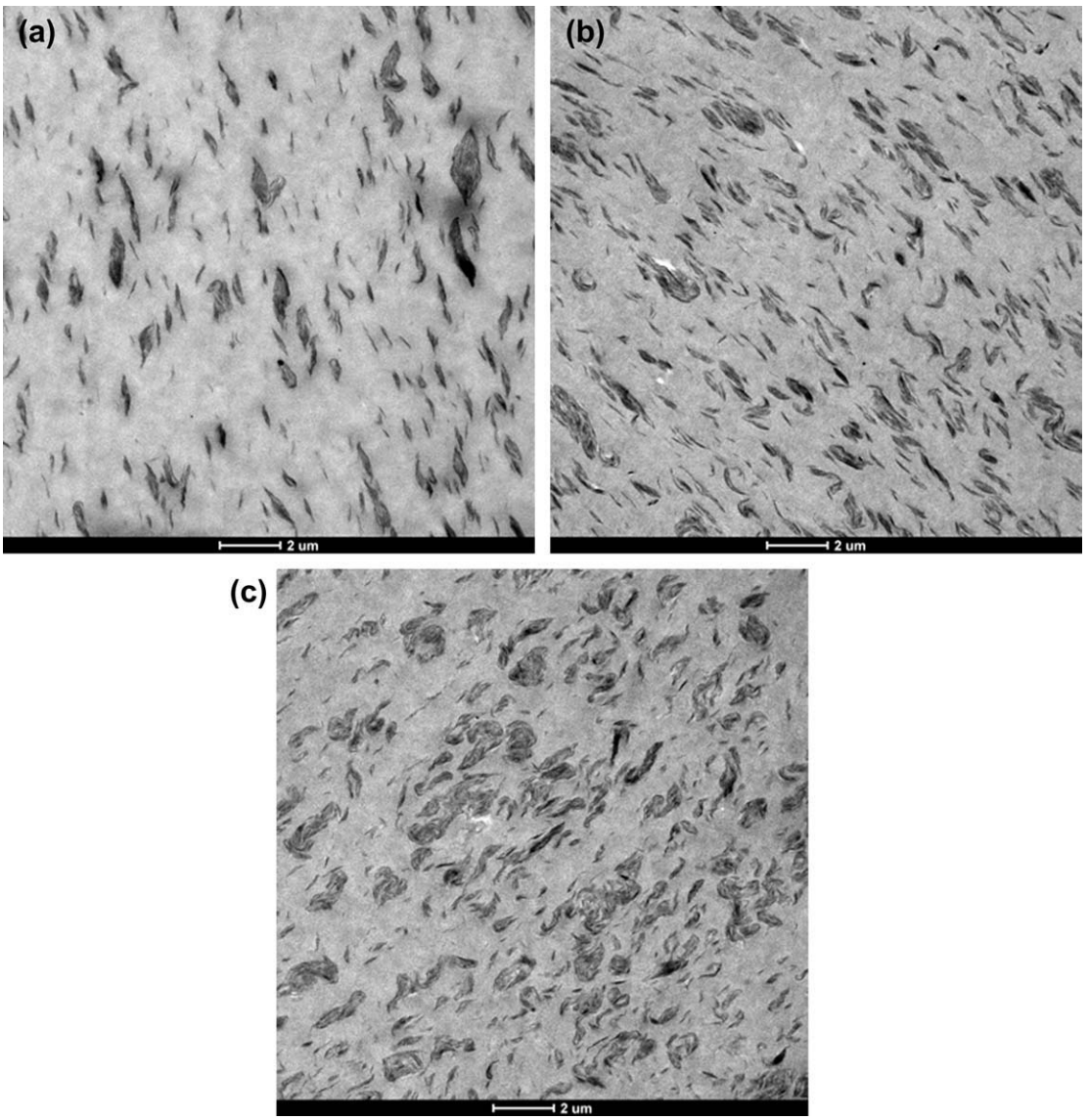

Figure 5 TEM micrographs of Nc's based on LDPE (a) and the 90/10 (b) and 80/20 (c) LDPE/Pema-Zn blends with 10% MMT.

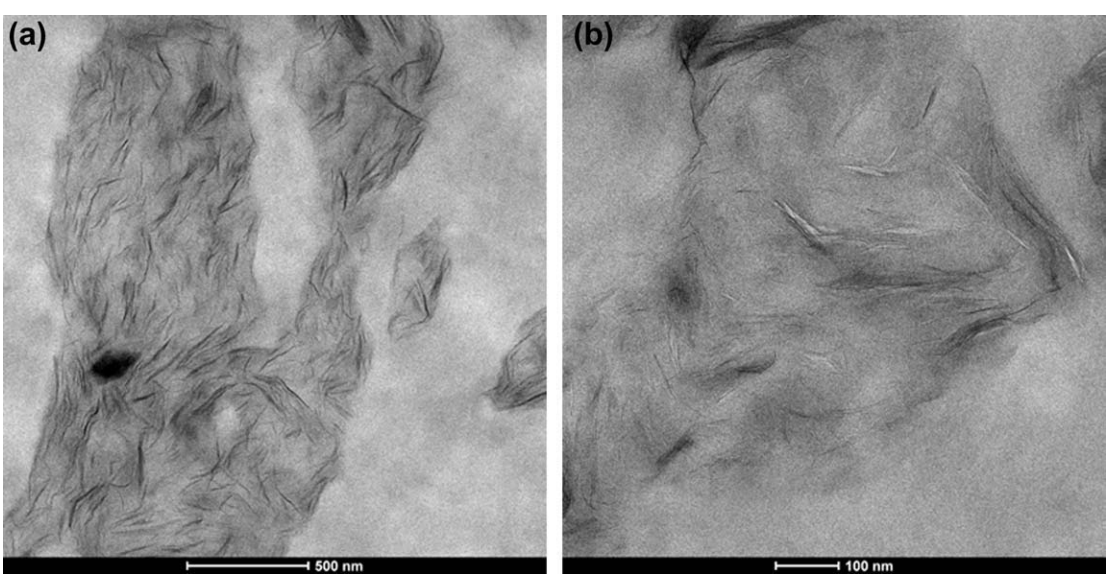

Figure 6 Detailed TEM micrographs of a typical domain with concentrated MMT (20/3 Nc) at low (a) and high (b) magnification.

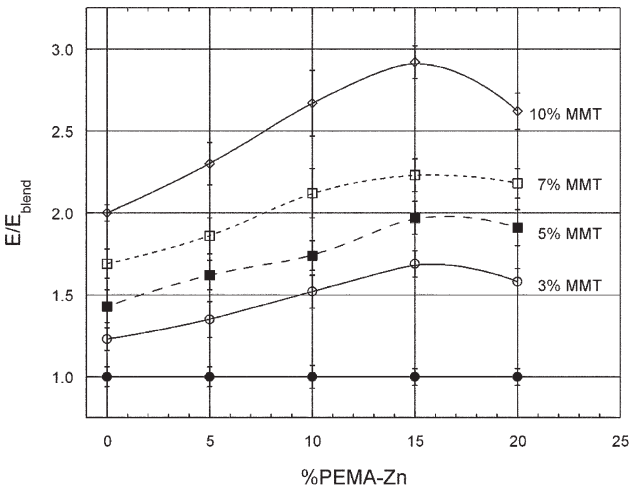

Figure 7 Modulus of the Nc's relative to that of the correspondent blend matrix as a function of the Pema-Zn content.

therefore, that the matrix of these Nc's is composed of a single mixed polymeric phase.

As expected, large MMT stacks are present in the LDPE of this work [Fig. 5(a)], because MMT does not exfoliate in PE. The interlaminar spacing corresponds to that measured by WAXS. If we compare Figure 5(a) (pure LDPE), Figure 5(b), and Figure 5(c) (Nc's modified with 10 and 20% Pema-Zn, respectively) the number of dispersed particles increased when 10% of Pema-Zn was added. Upon a further increase in the Pema-Zn content, the average particle size increased up to several microns, occupying roughly half the area of the micrograph [Fig. 5(c)]. Thus, the higher the Pema-Zn content, the greater the area occupied by the exfoliated/dispersed MMT. The same effect occurred at lower MMT contents.

The nanostructure of these surprisingly big particles can be determined by noting that the MMT does not expand throughout the whole matrix [Fig. 6(a)], but rather it is confined inside the large domains. Within them, MMT is largely dispersed in the form of thin platelets, or often as individual layers [Fig. 6(b)]. To our knowledge, this lack of full dispersion throughout the matrix, and the concentration of highly exfoliated MMT within irregular microscopic domains have not been reported to date. As the MMT tends to be located in the Pema-Zn because it is more compatible with it, a tentative explanation is that the location of the MMT particles is related to that of the ionic clusters that were not fully disrupted in the Nc's. Thus, MMT would be concentrated only in the zones where the ionic clusters are present. In this way Figure 6, and to a minor extent Figure 5, inform us about the location of the ionomer clusters inside the LDPE/Pema-Zn system. In this scenario, there would be a heterogeneous structure composed by a pure matrix, and zones where the same matrix, a large concentration of Pema-Zn clusters, and highly exfoliated nanoclay are present. To our knowledge, the location of Pema-Zn clusters has not been identified in previous studies, and would be difficult to locate by any other technique.

With respect to the mechanical performance of these new structures, it is expected that compatibility is assured since the ionomer is present throughout the whole system. It is not possible to know beforehand the effect that the reinforcement provided by a MMT concentration as high as that observed in Figure 6 will have (note that the MMT content of the Nc of Fig. 6 is only 3%). It appears that the sheets are less oriented than what is usually observed in injection molded Nc's. However, the fact that exfoliation of the MMT is important leads us to believe that there should be property increases characteristic of Nc's. This possibility will be studied in the next section.

Mechanical properties

The moduli of the Nc's relative to that of the corresponding blend matrix will provide a measure of the MMT dispersion throughout the whole specimens. For this reason they are collected in Figures 7 and 8 as a function of Pema-Zn and MMT contents, respectively. The modulus values are relative to those of the corresponding blend matrix; i.e., possible modulus changes due to the ionomer addition are not taken into account and, therefore, the modulus increases are solely due to the presence of MMT. Figure 7 reveals that increasing amounts of Pema-Zn (up to a 15%) led to modulus increases, regardless of the MMT content. Therefore, dispersion increases until a 15% Pema-Zn content is achieved, and then

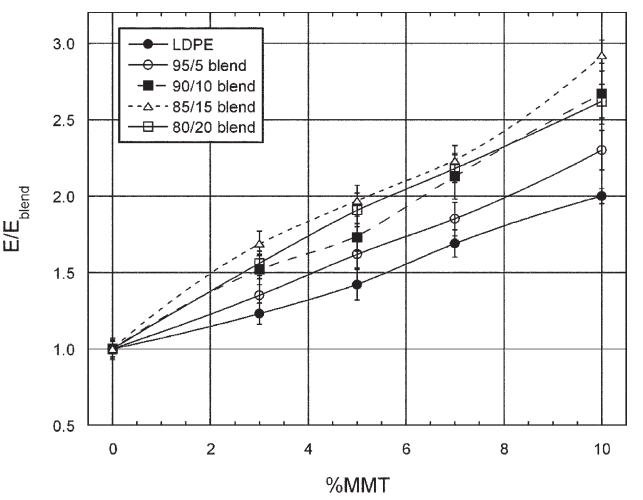

Figure 8 Modulus of the Nc's relative to that of the correspondent blend matrix as a function of the MMT content.

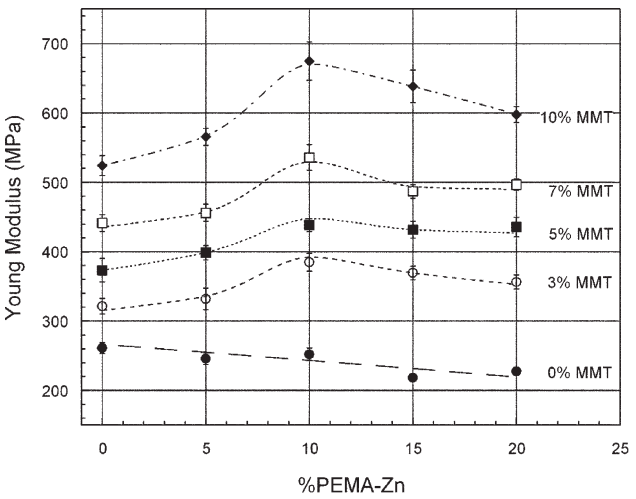

Figure 9 Absolute modulus of elasticity of the Nc's as a function of the MMT content.

decreases (as does the modulus) in the Nc's with 20% Pema-Zn. These differences in dispersion were not detected in the TEM micrographs, as the difference in dispersion is too small to be detectable in the small areas observed by TEM. Thus, 15%Pema-Zn appears as the optimum ionomer content in these systems. Moreover, this optimum amount is independent of the MMT content.

As expected, when the dependence of modulus on % MMT is analyzed (Fig. 8), modulus increases are observed with MMT content through out the range studied. As one would anticipate from the maximum observed in Figure 7, the curve for 15% Pema-Zn stays always above that of 20% Pema-Zn, regardless of the MMT content. Therefore, an increase in the modifier content to 20% is not positive for the modulus.

The absolute moduli of elasticity of the Nc's are shown in Figure 9. There are some characteristics that should be underlined. First, as seen in the curve for 0% MMT, the presence of Pema-Zn is slightly negative for the modulus of the blends, and therefore, of the Nc's. Second, the modulus increases with respect to that of the LDPE reach a 160% in the 10/10 Nc. When the significance of this increase is judged, it must be taken into account that low modulus matrices show comparatively larger modulus increases than those attained for example in engineering polymers. In Figure 9, increases in the MMT content led to modulus increases regardless of Pema-Zn content, indicating the positive effect of the MMT presence; third, the maximum in modulus occurs at a 10% Pema-Zn content. Therefore, as stated before, dispersion was the highest in the Nc's with 15% Pema-Zn, but as the ionomer addition decreases the modulus, the largest modulus value appears at lower Pema-Zn contents; i.e., at a 10% Pema-Zn content.

The performance of these LDPE based Nc's with an ionomer as modifier at a constant 5% MMT content, is compared with that of other modifiers used in polyolefins in Table II. The very low modulus reported in some cases,[16,19,40] led to unrealistic relative modulus increases; therefore the absolute modulus increases are reported. The absolute modulus increases are reported with respect to that of the neat polymer, and also to that of the blend matrix (these values are related to dispersion). Four different compatibilizers are collected. As the amount of papers that use maleic anhydride grafted modifiers is very large, the papers with the largest and lowest increases reported, as well as that with an unusual PE-g-MA content, are collected. As can be seen, the performance of the ionomer studied in this paper, together with that of PE-g-MA, are clearly the best reported. The rest of the compatibilizers clearly showed a lesser compatibilizing effect. If we look at the absolute modulus, even the modulus increase provided by the ionomer of this study is comparatively higher. This comparison shows the ability of

TABLE II
Absolute Modulus Improvements and Ductility of Various Systems Based on Polyethylene, with Different Compatibilizers and with 5% MMT

Polymer	Organoclay	Compatibilizer (content, %)	Absolute modulus increase with respect to the pure polymer (MPa)	Absolute modulus increase with respect to the polymer/ compatibilizer blend matrix (MPa)	Ductility decrease with respect to the pure matrix (%)	Reference
LLDPE	Cloisite 20A	LLDPE-g-MA (10%)	290	264	0	14
LLDPE	Cloisite 20A	LLDPE-g-MA (15%)	41	41	+47	16
HDPE	Cloisite 20A	HDPE-g-MA (50%)	118	82	–	40
LLDPE	Cloisite 20A	Zn ionomer (18%)	106[a]	–	−10	18
LLDPE	Cloisite 20A	Ox-PE (10%)	100	–	−20[a]	19
LDPE	Cloisite 15A	PE-co-methyl acrylate (15%)	14	–	+9	28
LDPE	Cloisite 20A	Zn ionomer (10%)	177	186	−10	this work

[a] Interpolated value

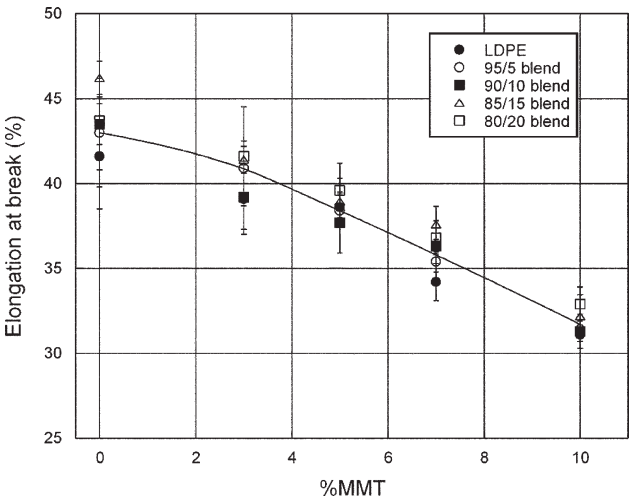

Figure 10 Elongation at break of the Nc's as a function of the MMT content.

the used Pema-Zn ionomer to disperse and compatibilize LDPE based Nc's.

The ductility of the Nc's measured by the elongation at break is shown in Figure 10 as a function of the MMT content. The decreases observed are low. This is because the maximum decrease in the Nc's with a 10% MMT was only 24%. Furthermore, the ductility of the Nc's does not depend on the Pema-Zn content. This is probably related to the fact that the ductility decrease was also low in the case of the Nc's without compatiblizer. The last column of Table II demonstrates that this behavior is common in the case of polyethylene, and it is attributed to their rubbery nature.

CONCLUSIONS

The Pema-Zn is mixed in a single phase with the LDPE-based matrix up to contents of at least 20%, as no evidence of a second phase is observed by TEM. The increase in tan δ at roughly 25°C (where the peak of Pema-Zn occurred) suggests the presence of some ionic groups in the Nc's typical of ionomers.

The MMT appears concentrated in dispersed and irregular microscopic domains that occupy the surface of the Nc's observed by TEM. This structure has not been previously observed to our knowledge. As the MMT is prone to be located close to the Pema-Zn because of its higher compatibility, it is plausible that the zones where the MMT is located are also the zones where the ionic clusters of the Pema-Zn are concentrated.

The MMT was rather well dispersed in the form of thin platelets or individual layers. The heterogeneous location of the MMT was not negative for the mechanical response of the Nc's since the observed modulus increases were among the highest reported to date. The maximum dispersion occurred in the Nc's with 15% Pema-Zn (maximum modulus increase with respect to the modulus of the blend matrix). The absolute maximum modulus increase with respect to the LDPE modulus occurred (due to the lower modulus of the ionomer) in the Nc with 10% Pema-Zn and reached 670 MPa; i.e., a 160% increase with 10% MMT.

The technical support of the Polymer Characterization Service of the University of Basque Country for the TEM analysis is gratefully acknowledged. P. Santamaría acknowledges the grant awarded by the Basque Government.

References

1. Utracki, L. A.; Clay-Containing Polymeric Nanocomposites; Rapra Technology, Ltd.: Shropshire 2004.
2. Paul, D. R.; Robeson, L. M. Polymer 2008, 49, 3187.
3. Fornes, T. D.; Yoon, P. J.; Hunter, D. L.; Keskkula, H.; Paul, D. R. Polymer 2002, 43, 5915.
4. Gurmendi, U.; Eguiazabal, J. I.; Nazabal, J. Compos Sci Technol 2006, 66, 1221.
5. Yoo, Y.; Paul, D. R.; Polymer 2008, 49, 3795.
6. Gonzalez, I.; Eguiazabal, J. I.; Nazabal, J. Polym Eng Sci 2006, 46, 864.
7. Gonzalez, I.; Eguiazabal, J. I.; Nazabal, J. Polymer 2005, 46, 2978.
8. Shah, R. K.; Paul, D. R. Polymer 2004, 45, 2991.
9. Seong, W. K.; Won, H. J.; Moo, S. L.; Moon, B. K.; Jae, Y. J. Polymer 2001, 42, 9837.
10. Lepoittevin, B.; Pantoustier, N.; Devalckenaere, M.; Alexandre, M.; Calberg, C.; Jérôme, R.; Henrist, C.; Rulmont, A.; Dubois, P. Polymer 2003, 44, 2033.
11. Chisholm, B. J.; Moore, R. B.; Barber, G.; Khouri, F.; Hempstead, A.; Larsen, M.; Olson, E.; Kelley, J.; Balch, G.; Caraher, J. Macromolecules 2002, 35, 5508.
12. Colonna, M.; Berti, C.; Binassi, E.; Fiorini, M.; Karanam, S.; Brunelle, D. J. Eur Polym J 2010, 46, 918.
13. Vidotti, S. E.; Chinellato, A. C.; Hu, G. H.; Pessan, L. A. J Polym Sci Part B: Polym Phys 2007, 45, 3084.
14. Hotta, S.; Paul, D. R. Polymer 2004, 45, 7639.
15. Wang, K. H.; Choi, M. H.; Koo, C. M.; Choi, Y. S.; Chung, I. J. Polymer 2001, 42, 9819.
16. Zhang, M. Q.; Sundararaj, U. Macromol Mater Eng 2006, 291, 697.
17. Morawiec, J.; Pawlak, A.; Slouf, M.; Galeski, A.; Piorkowska, E.; Krasnikowa, N. Eur Polym J 2005, 41, 1115.
18. Sanchez-Valdes, S.; Lopez-Quintanilla, M. L.; Ramirez-Vargas, E.; Medellin-Rodriguez, F. J.; Gutierrez-Rodriguez, J. M. Macromol Mater Eng 2006, 291, 128.
19. Luyt, A. S.; Geethamma, V. G. Polym Test 2007, 26, 461.
20. Durmus, A.; Kasgoz, A.; Macosko, C. W. Polymer 2007, 48, 4492.
21. Geethamma, V. G.; Luyt, A. S. J Nanosci Nanotech 2008, 8, 1886.
22. Durmus, A.; Woo, M.; Kasgoez, A.; Macosko, C. W.; Tsapatsis, M. Eur Polym J 2007, 43, 3737.
23. Minkova, L.; Peneva, Y.; Tashev, E.; Filippi, S.; Pracella, M.; Magagnini, P. Polym Test 2009, 28, 528.
24. Picard, E.; Vermogen, A.; Gérard, J. F.; Espuche, E. J Polym Sci Part B: Polym Phys 2008, 46, 2593.
25. Chinellato, A. C.; Vidotti, S. E.; Hu, G.-H.; Pessan, L. A. J Polym Sci Part B: Polym Phys 2008, 46, 1811.
26. Chrissopoulou, K.; Altintzi, I.; Anastasiadis, S. H.; Giannelis,

E. P.; Pitsikalis, M.; Hadjichristidis, N.; Theophilou, N. Polymer 2005, 46, 12440.
27. Scaffaro, R.; Botta, L.; La Mantia, F. P. Macromol Mater Eng 2009, 294, 445.
28. Golebiewski, J; Rozanski, A.; Dzwonkowski, J.; Galeski, A. Eur Polym J 2008, 44, 270.
29. Santamaría, P.; Eguiazábal, J. I.; Nazábal, J. J Appl Polym Sci 2010, 116, 2374.
30. Tadano, K.; Hirasawa, E.; Yamamoto, H.; Yano, S. Macromolecules 1989, 22, 226.
31. Perrin Sarazin, F.; Ton That, M. T.; Bureau, M. N.; Denault, J. Polymer 2005, 46, 11624.
32. Popli, R.; Glotin, M.; Mandelkern, L. J Polym Sci Part B: Polym Phys 1984, 22, 407.
33. Boyd, R. H. Polymer 1985, 26, 1123.
34. Tachino, H.; Hara, H.; Hirasawa, E.; Kutsumizu, S.; Tadano, K.; Yano, S. Macromolecules 1993, 26, 752.
35. Kutsumizu, S.; Tadano, K.; Matsuda, Y.; Goto, M.; Tachino, H.; Hara, H.; Hirasawa, E.; Tagawa, H.; Muroga, Y.; Yano, S. Macromolecules 2000, 33, 9044.
36. Xie, Y.; Yu, D.; Kong, J.; Fan, X.; Qiao, W. J Appl Polym Sci 2006, 100, 4004.
37. Shah, R. K.; Cui, L.; Williams, K. L.; Bauman, B.; Paul, D. R. J Appl Polym Sci 2006, 102, 2980.
38. Goitisolo, I.; Eguiazábal, J. I.; Nazabal, J, Polym Adv Tech 2009, 20, 1060.
39. Mainil, M.; Alexandre, M.; Monteverde, F.; Dubois, P. J Nanosci Nanotech 2006, 6, 337.
40. Lee, Y. H.; Park, C. B.; Sain, M.; Kontopoulou, M.; Zheng, W. J Appl Polym Sci 2007, 105, 1993.